Current Research in Food Science 5 (2022) 581–589

Contents lists available at ScienceDirect

Current Research in Food Science

journal homepage: www.sciencedirect.com/journal/current-research-in-food-science

The role of probiotic exopolysaccharides in adhesion to mucin in different gastrointestinal conditions

Yanmeng Lu [a,1], Shengyi Han [a,1], Shuobo Zhang [a], Kaicen Wang [a], Longxian Lv [a], David Julian McClements [b], Hang Xiao [b], Björn Berglund [a,c], Mingfei Yao [a,**], Lanjuan Li [a,*]

[a] State Key Laboratory for Diagnosis and Treatment of Infectious Diseases, National Clinical Research Center for Infectious Diseases, Collaborative Innovation Center for Diagnosis and Treatment of Infectious Diseases, The First Affiliated Hospital, Zhejiang University School of Medicine, Hangzhou, 310003, China
[b] Department of Food Science, University of Massachusetts, Amherst, MA, 01003, USA
[c] Department of Biomedical and Clinical Sciences, Linköping University, Linköping, SE, 58183, Sweden

ARTICLE INFO

Keywords:
Exopolysaccharides (EPS)
Mucoadhesion
Adhesion force
Lactobacillus rhamnosus GG
Pediococcus pentosaceus LI05

ABSTRACT

The presence of exopolysaccharides (EPS), a type of biomacromolecules, on the surface of probiotics play an important role in mucoadhesion, and it can be severely influenced by environments during gastrointestinal transit. In this study, the impact of gastrointestinal factors on surface properties of two probiotics (*Lactobacillus rhamnosus* GG and *Pediococcus pentosaceus* LI05) was investigated. Probiotic suspensions had relatively high viscosities and exhibited pronounced shear-thinning behavior due to the presence of EPS. The ζ-potential of both probiotics was relatively low and was not believed to play an important role in mucoadhesion. Compared to the control, the adhesive forces tended to decrease in the presence of gastric acids but increase in the presence of bile salts, since bile salts led to a thicker more open EPS layer compared to gastric acids. Although the functional groups of EPS in both probiotics are similar according to the study by FT-IR spectroscopy, the molecular weight of purified EPS in LI05 was much higher, ranging from 10,112 Da to 477,763 Da, which may contribute to higher rupture length in LI05 group. These results suggest that probiotic-mucin interactions are governed by the compositions and changes in the EPS of the probiotics in different gastrointestinal conditions, which contribute to a better understanding of the mucoadhesive behavior of the probiotics in the GIT.

1. Introduction

Exopolysaccharides (EPS) are extracellular biopolymers produced by many microorganisms, including bacteria, fungi and cyanobacteria, to protect the microbial cells from varied environmental stresses (Zhou et al., 2019). They can either attach to the envelope of the bacteria as a loose layer or can be directly secreted into the environment as mucus (Rahbar Saadat, Yari Khosroushahi and Pourghassem Gargari, 2019). The nature of bacterial EPS mainly depends on strains, medium composition and culture conditions. The different EPS usually varied in monosaccharide composition, charge, connections between units, and the presence of repeated side-chains and substitutions (Ciszek-Lenda, 2011; Rahbar Saadat, Yari Khosroushahi and Pourghassem Gargari, 2019). EPS affect the surface properties of the probiotics, especially mucoadhesion of bacterial cells in the gastrointestinal tract (GIT). For instance, EPS enhanced the hydrophobicity of bacterial cell surface, which increase the ability of bacteria to bind to intestinal mucosa (Sun et al., 2007). Besides, they also promote biofilm formation, increasing the chances of bacterial survival in the GIT and contributing to the colonization of epithelial cells (Konieczna et al., 2018; Lebeer et al., 2009).

The mucoadhesive ability of probiotics is an important factor contributing to their ameliorative effects since it facilitates colonization of the intestines and inhibits the adhesion of pathogenic bacteria (Kumar & Kumar, 2015). Indeed, mucoadhesion is assumed to be a prerequisite for the beneficial health effects of these probiotics (Van Tassell and Miller, 2011). *Lactobacillus rhamnosus* GG (LGG), as one of the most documented lactic acid bacteria (LAB) used in food strains, has been demonstrated to produce unique bacterial pili that produce mucus-binding proteins that enhance its mucoadhesive function

* Corresponding author.
** Corresponding author.
E-mail addresses: mingfei@zju.edu.cn (M. Yao), ljli@zju.edu.cn (L. Li).
[1] Co-first authors.

https://doi.org/10.1016/j.crfs.2022.02.015
Received 1 February 2022; Received in revised form 19 February 2022; Accepted 28 February 2022
Available online 16 March 2022

(Kankainen et al., 2009; von Ossowski et al., 2010). Pilus-mediated adhesion may strengthen the bacteria-host interaction, whereas EPS on LGG surfaces may have interfering effects on these interactions (Tripathi et al., 2013).

After oral administration, the viability of probiotics may be severely reduced by the harsh conditions in the different regions of the GIT, such as high concentrations of gastric acids, bile salts, and digestive enzymes (Han et al., 2021; M. F. Yao, Xie, Du, McClements, Xiao and Li, 2020). Moreover, after viable probiotics reach the colon, they must also successfully colonize the intestinal mucosa in competition with indigenous bacteria (Zmora et al., 2018). Hence, it is important to understand how key gastrointestinal constituents, such as gastric acids and bile salts, affect the mucoadhesive properties of probiotics. Indeed, several studies have shown that the survivability of lactic acid bacteria in low pH and when exposed to bile salts are highly variable (Reale et al., 2015). A number of different structures on the surfaces of *Lactobacilli* bacteria have been demonstrated to contribute to their mucoadhesive properties, implying that this species can adapt to the constantly changing intestinal environment of the host (Nishiyama et al., 2016).

We recently showed that *Pediococcus pentosaceus* LI05 (CGMCC 7049) isolated from fecal samples of a healthy volunteer exhibited acid- and bile-tolerant traits. However, the molecular mechanisms of mucoadhesion of LI05 have not been elucidated. In this study, we hypothesized that simulated gastrointestinal fluids could affect physicochemical property of EPS, thus influencing the mucoadhesive effects of LGG and LI05. Our hypothesis was verified by evaluating their viscosity, electrical, morphological and mucoadhesion properties of LGG and LI05 in simulated gastrointestinal conditions.

2. Materials and methods

2.1. Bacterial strains

LI05 and LGG (ATCC 53103) strains were used as model probiotics in this study. LI05 was originally isolated from the feces of healthy volunteers (Lv et al., 2014; Shi et al., 2017). Bacterial strains were stored in MRS broth (Difco, BD, Sparks, MD, USA) supplemented with 20% glycerol at −80 °C. They were cultured anaerobically in MRS broth for 24 h at 37 °C separately before usage in the experiments. The isolated bacteria (1800 rcf for 5 min) were washed three times and then stored at 4 °C before analysis. The cells were washed with saline buffer and gently blowing with a pipette gun at a rate of 60 beats per minute for 20 s.

2.2. Preparation of probiotic cell suspensions

LI05 and LGG were cultivated in MRS medium, centrifuged at 1800 rcf for 5 min, and then the pellets were collected. Gastric acid (GA) and bile salt (BS) solutions, designed to simulate the fluids found in the stomach and small intestine (but without the digestive enzymes) were prepared according to the methods described previously, with a few modifications (Brodkorb et al., 2019; M. Yao, Wu, Li, Xiao, McClements and Li, 2017). The GA (1 L) contained 2 g of sodium chloride, 7 mL of 1 M hydrochloric acid, and 3.2 g of pepsin and was adjusted to pH 2.5. The BS (1 L) contained 8.8 g of sodium chloride and 5.0 g of bile salts. Then, 9 ml of gastric acid, bile salt, or phosphate buffered saline (PBS) solutions were pre-incubated separately in a constant temperature shaker at 37 °C and 100 rpm for 30 min. Afterwards, 1 ml (10 Log CFU/ml) of LI05 or LGG suspension was added to the above-mentioned solutions in equal amounts (1:1 v/v) and the resulting samples are designated as LGG-GA, LGG-BS, LGG-Ctrl, LI05-GA, LI05-BS and LI05-Ctrl, respectively. After 10 min, the solutions were transferred to a constant temperature shaker (37 °C) under the same stirring conditions as described earlier, after which the appearance and optical densities (ODs) of the different probiotic suspensions (GA, BS and PBS) were recorded. The OD values were measured using a microplate reader (LabSystems Multiskan MS, Labsystems Diagnostics Oy, Vantaa, Finland) at a wavelength of 630 nm. The gastric acid samples were then neutralized to pH 7.0 by adding 1% NaOH solution (Sigma-Aldrich, Saint Louis, MO, USA). After centrifugation at 1800 rcf for 5 min, the probiotic suspensions were washed twice with PBS solution then their viscosities and ζ-potential values were analyzed with the concentration of 10 Log CFU/ml within 4 h.

2.3. Viscosity measurements

The apparent shear viscosity of the probiotic suspensions was determined using a rotary rheometer (HAAKE MARS III, Thermo Fisher Scientific, Karlsruhe, Germany). Samples were placed in the concentric cylinder at ambient temperature and the shear stress was measured as the shear rate was increased from 0.1 to 100 s^{-1}. The apparent shear viscosity *versus* shear rate profiles were then calculated from this data.

2.4. Zeta-potential measurements

The effective surface potential, expressed as the ζ-potential, of the probiotic cells was measured using a particle electrophoresis device (Zeta-sizer, Malvern Panalytical, Malvern, UK). The cell suspensions were diluted with PBS (0.1 M, pH 7.0) prior to analysis to ensure that the light scattering signal was in an appropriate range for measurements. The sign and magnitude of the ζ-potential were then determined from the direction and velocity that the cells moved in an applied electrical field.

2.5. Scanning electron microscopy

The MRS medium used for cultivation of the LI05 and LGG was centrifuged at 1800 rcf for 5 min and the supernatant was discarded. After rinsing the cells twice with PBS solution and centrifuging (1800 rcf for 5 min), the microstructure of the separated probiotics was visualized using scanning electron microscopy (SEM).

Samples for SEM were prepared according to the following steps: a) *Fixation*: the probiotic suspension was first fixed with 2.5% glutaraldehyde in PBS solution (0.1 M, pH 7.0) for more than 4 h. These samples were then washed three times in PBS (0.1 M, pH 7.0) for 15 min at each step. Subsequently, the samples were fixed with 1% OsO_4 in phosphate buffer for 1–2 h and washed three times in phosphate buffer (0.1 M, pH 7.0) for 15 min at each step. b) *Dehydration*: the sample was first dehydrated with aqueous ethanol solutions with increasing ethanol concentrations (30%, 50%, 70%, 80%, 90%, and 95%) for about 15 min at each step. They were then dehydrated twice using pure ethanol for 20 min at each step or stored in ethanol. The samples were then dehydrated using a critical point dryer (Hitachi Model HCP-2, Tokyo, Japan). c) *Coating and observation*: the dehydrated samples were coated with gold-palladium using an ion sputter device (Hitachi Model E−1010, Tokyo, Japan) for 4–5 min and then their microstructures were observed using scanning electron microscopy (Hitachi Model SU-8010 SEM, Tokyo, Japan).

2.6. Atomic force microscopy

2.6.1. Preparation of mucin-modified AFM tips

Atomic force microscopy (AFM) probes (CP-qp-Scont Nanosensors, Watsonville, CA, USA) with borosilicate glass beads (1.5 μm) were functionalized with mucin. Before preparing the mucin-modified tips, the cantilever spring constant was calibrated using a thermal K method program equipped with IGOR Pro 6.04 (Wavemetrics, Osewego, OR, USA). The spring constant of the probes was 0.01 nN/Nm. Initially, the tips were put in a PSD-UV UV-ozone cleaner (Novascan, Phoenix, AZ, USA) for 8 h, immersed in a 1% ethanol solution for 4 h, rinsed with deionized water, and then immersed in a 10% glutaraldehyde aqueous solution for 2 h and washed with deionized water. Then, the tips were immersed in a solution containing 2 mg/ml porcine gastric mucus (Sigma Aldrich, St. Louis, MO). After incubation for 8 h, the tips were

placed in PBS solution.

2.6.2. Preparation of bacterial surface

After incubation in GA, BS or PBS solutions, the LGG and LI05 suspensions were deposited on cationic polylysine-modified slides and incubated at 4 °C for 4 h. After the bacterial cells adhered to the glass slides, they were rinsed gently with PBS solution twice. Finally, the AFM tips were rinsed with milli-Q-grade water before use.

2.6.3. Atomic force microscopy analysis

The microstructure of the probiotics was also analyzed in a saline buffer solution (pH 7.0) at 25 °C using an atomic force microscope (Asylum MFP-3D, Santa Barbara, CA, USA). Image acquisition and analysis was carried out using the operating software (IGOR Pro 6.04, Wavemetrics). For each experiment, the probe tips were moved over the bacterial surface in the microscope's field-of-view using a fixed scanning area of 5 μm × 5 μm, a resolution of 16 × 16 corresponding to 32 × 32 points (1024 force curves), a loading force of 1 nN, a needle approach and retraction speed of 400 nm/s, and a contact time of 2 s when the probe touched the bacterial surfaces. Each sample was analyzed four times.

2.7. Quantification of EPS on the surface layer of probiotic cells

The EPS concentration of the probiotics was quantified using an enzyme-linked immunosorbent assay (ELISA) (Runyu Biological Technology Co., Shanghai, China) according to the manufacturer's instructions. Briefly, 10 ml of each probiotic suspension (~10^7 CFU) was centrifuged at 3200 rcf for 15 min and the supernatant was collected for further measurements. Solid-phase antibodies were made by coating a microtiter plate with purified EPS antibodies. Then, 50 μl EPS solution was added to the microwells, after which the added EPS was labeled with horseradish peroxidase (Pierce Biotechnology, Rockford, IL, USA). After about 30 min, the antibodies formed antibody-antigen-enzyme-labeled antibody complexes. The plate was then washed and the substrate tetramethylbenzidine (TMB) was added for color development. TMB is converted into blue through catalysis facilitated by horseradish peroxidase and then changes into a yellow color when exposed to acid. The color intensity produced is proportional to the quantity of EPS in the sample. Finally, the OD value was measured with a microplate reader (LabSystems Multiskan MS, Labsystems Diagnostics Oy) at 450 nm. The concentration of EPS in the sample was calculated from a standard curve.

2.8. Molecular weight analysis and Fourier Transform-Infrared (FT-IR) spectroscopy of ESP

This EPS was isolated and purified according to previous the research, and the crude EPS was first extracted by a cold ethanol precipitation method (Bramhachari and Dubey, 2006). Then the crude EPS was re-dissolved in distilled and deionized water and fractionated by ion-exchange chromatography on a DEAE-Sepharose Fast-Flow (Pharmacia, Piscataway NJ, USA). The column was eluted with deionized water and sodium chloride solution (Cao et al., 2021). Elution was collected every 10 min through an autosampler (Borui, Yangzhou, China) and evaluated for total carbohydrate content. Then, the peak fractions containing EPS were concentrated, dialyzed, lyophilized and purified by gel filtration chromatography via a SephacrYL-300 column (1.6 mm × 60 mm, GE Healthcare, USA).

The molecular weight (Mw) of the EPS was measured by High Performance Gel Permeation Chromatography (HPGPC, LC10A, Shimadzu, Japan) equipped with a differential detector (RI-502, *Shodex*, Tokyo, Japan). 100 μg of EPS was dissolved in 2 ml 0.05 M NaCl and filtered with a 0.2 μm microporous membrane filter (Sartorius Australia, Oakleigh, Victoria, Australia) before being added into a BRT105–104-102 (BoRui Saccharide, Yangzhou, China) column (8.0 mm × 300 mm), with a flow rate of 0.6 mL/min. Molecular weight was calculated according to the standard curve.

The FT-IR spectrum of EPS was recorded on an FT-IR 650 (Gangdong, Tianjin, China). About 2 mg of EPS powder were mixed well with 200 mg KBr powder, and then put into 1-mm thick pellets and pressed. The spectrum was recorded in 4000–400 cm^{-1} and analyzed by the FT-IR 650 software (Gangdong, Tianjin, China).

2.9. Statistical analysis

A Kolmogorov–Smirnov test was used to analyze whether the data followed a normal distribution. The Mann-Whitney test was used for data that were not normally distributed, whereas the one-way ANOVA with Bonferroni's multiple comparison test performed *post hoc* was used for normally distributed data in order to determine the statistical significance. Results were expressed as means ± standard errors. Statistical analyses were conducted using R software (v.2.15.3) and SPSS (v.20.0). Images were constructed with Graph-Pad Prism (v.8.0), R software (v.2.15.3), and Adobe Illustrator (v.cc2020). Two-tailed P-values < 0.05 were considered statistically significant.

3. Results and discussion

3.1. Impact of simulated gastrointestinal fluids on probiotic properties

Probiotics traveling through the GIT are surrounded by fluids containing different gastrointestinal constituents depending on the region of the GIT, such as gastric acids in the stomach and bile salts in the small intestine (Johansson et al., 2011; Nishiyama et al., 2016). These changes in the composition of the gastrointestinal fluids may alter the physicochemical properties of the probiotic suspensions, such as their aggregation state, viscosity, and surface charge. Changes in these parameters may then alter the retention time and behavior of the probiotics in the different regions of the GIT by altering their adhesion to the mucus layer coating the epithelium cells. For this reason, we measured changes in the optical density, viscosity, and surface potential of the probiotics in different simulated GIT fluids.

3.1.1. Optical density

The optical density of the LGG and LI05 suspensions depended on the nature of the solutions used to suspend them: PBS, GA or BS (Fig. 1a). Compared to the controls, the OD values of the probiotic suspensions were slightly higher for the gastric acid solutions but slightly lower for the bile salt solutions (Fig. 1a). These results suggest that there were changes in the size, aggregation state, and/or refractive index of the probiotic cells in the different solutions. On the other hand, there were no major changes in the overall appearance of the probiotic cell suspensions in the different solutions (Fig. 1a).

3.1.2. Shear viscosity

The apparent shear viscosity of the different probiotic suspensions was then measured as a function of shear rate to provide further information about the impact of gastrointestinal conditions on probiotic properties (Fig. 1b). All of the probiotic suspensions exhibited pronounced shear-thinning behavior, as seen by the large reduction in apparent shear viscosity with increasing shear rate. The suspensions also had a relatively high viscosity at low shear rates (>100 mPa s), which can mainly be attributed to the presence of extended EPS and the close packing of the probiotic cells. For LI05, the nature of the simulated gastrointestinal fluids did not have a major impact on the shear viscosity profiles of the probiotic suspensions (Fig. 1c). In contrast, for LGG, there was a pronounced increase in viscosity at intermediate shear rates for the probiotics in bile salt solutions and a slight increase in gastric acid solutions (Fig. 1b). These results suggest that the bile salts and gastric acids may have promoted some aggregation of the probiotic cells within the suspensions.

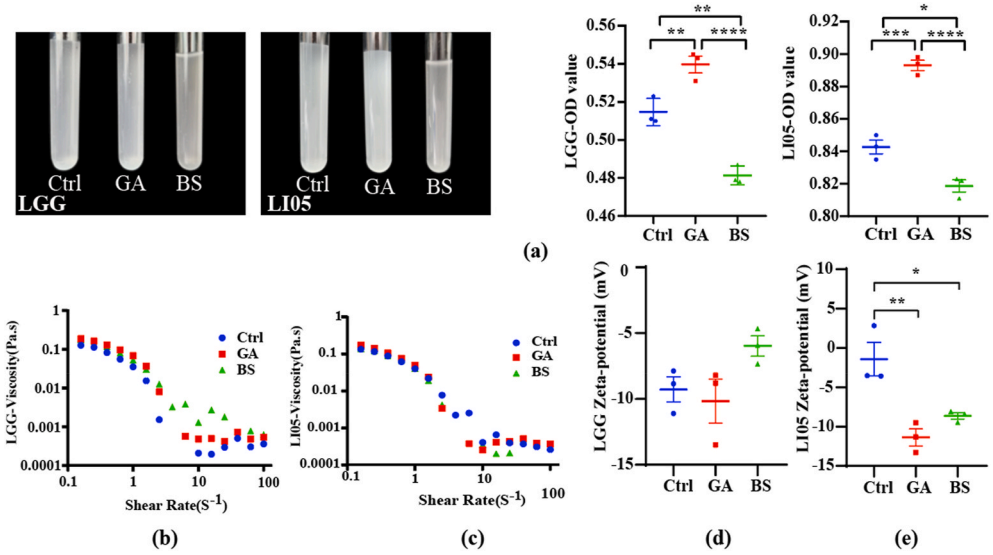

Fig. 1. The optical density value, apparent viscosity and ζ-potential of LGG and LI05. (a) The transmittance and optical density value of two probiotics (LGG and *P. pentosaceus* LI05) under different, simulated gastrointestinal conditions. The apparent viscosity of LGG (b) and *P. pentosaceus* LI05 (c) were measured with the shear rate ranging from 0.1 s^{-1} to 100 s^{-1}. The ζ-potential of LGG (d) and *P. pentosaceus* LI05 (e) were measured under different simulated gastrointestinal conditions. Ctrl, GA and BS represent different groups in the conditions of PBS, gastric acid and bile salts. Significant differences are indicated as follows: *P < 0.05, **P < 0.01, ***P < 0.001, ****P < 0.0001.

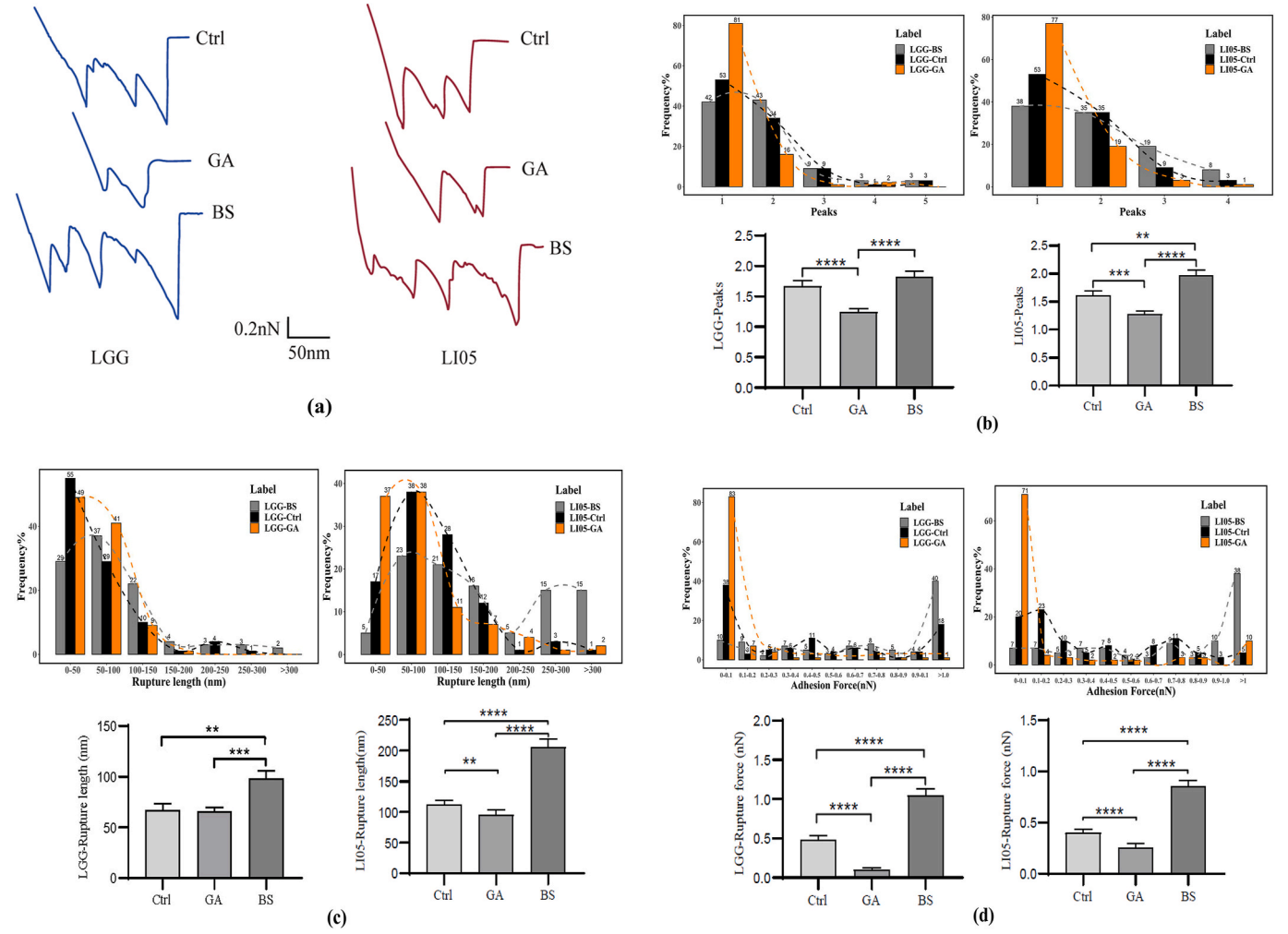

Fig. 2. Adhesion curves between probiotic and mucin measured by AFM. (a). Typical force curves of LGG-mucin and LI05-mucin selected from repeated experiments. The histograms displaying number of rupture peaks (b), rupture length (c), and adhesion forces (d) were obtained by recording force curves between mucin tips and probiotic cells under different, simulated gastrointestinal conditions. The dotted line represents a Gaussian fit of the data. The boxes and error bars denote means ± SEM (n = 100 force curves). Ctrl, GA and BS represent different groups in the conditions of PBS, gastric acid and bile salts. Significant differences are indicated as follows: *P < 0.05, **P < 0.01, ***P < 0.001, ****P < 0.0001.

3.1.3. ζ-Potential

Bacterial cell surfaces typically carry a negative charge (Halder et al., 2015). In this study, the probiotic cells were all negatively charged but the magnitude of their effective surface potentials depended on their environment. The ζ-potential of LGG cells in GA (−10.17 ± 1.67 mV) and BS (−5.97 ± 0.77 mV) solutions were different from those in the control solution (−9.27 ± 0.96 mV), but there were no statistical differences between these treatments. In contrast, the ζ-potential values of the LI05 cells suspended in GA (−11.4 ± 1.1 mV) and BS (−8.64 ± 0.41 mV) solutions were significantly more negative ($P < 0.05$) than those in the control group (−1.42 ± 2.13 mV). These results suggest that the gastric acids and bile salts changed the composition and/or ionization state of the surfaces of the probiotics. For instance, anionic bile salts may have adsorbed to the surfaces of the probiotics, thereby increasing their negative charge.

3.2. Adhesion curves between probiotics and mucin

The mucus layer covering the GIT is the first point of contact between the gut microbiota and the host (Johansson et al., 2008; Xu et al., 2021). The surfaces of probiotics contain numerous kinds of biological molecules and structures that impact their ability to attach to the mucus layer, including EPS, pili, and lipoteichoic acid (Konieczna et al., 2018; Lv et al., 2014; Proft and Baker, 2009). For this reason, insights into probiotic-mucin interactions under different gastrointestinal conditions were obtained by measuring adhesion curves using AFM.

3.2.1. Rupture peaks

As shown in Fig. 2a, the adhesion curves observed during retraction of the probiotics away from the mucus layer followed a worm-like-chain (WLC) model, which can be used to provide valuable information about the number of rupture events, the rupture length, and the rupture force (Burgain et al., 2015; Tripathi et al., 2013). Rupture peaks represent the contact points between the probiotic surfaces and mucin layer. For LGG, the ranking of rupture peak numbers between probiotic and mucin was as follows: LGG-GA (1.24 ± 0.06) < LGG-ctrl (1.67 ± 0.09) < LGG-BS (1.82 ± 0.09) (Fig. 2b). The rupture events observed for LI05-mucin under different gastrointestinal conditions displayed a similar trend as for LGG-mucin. No significant differences in rupture event numbers were observed between the two strains under different conditions. For LGG and LI05, nearly 80% of the adhesion curves observed under gastric acid treatment contained only one rupture peak (Fig. 2b), whereas for the group exposed to bile salts and the control group, a single rupture peak was observed in about 40% of the adhesion curves, with the remainder containing more than one rupture peak.

3.2.2. Rupture length

The rupture length represents the detachment of the probiotic surface layer from the AFM tips. For LGG, the average contour lengths (L_C) obtained from the probiotic-mucin retraction curves were 67.3 ± 5.9 nm for the control, 66.1 ± 3.5 nm for the GA sample, and 98.0 ± 7.9 nm for the BS sample (Fig. 2c). The frequency distribution plots showed that the majority of contour lengths were below 200 nm in all the samples. These contour lengths have similar dimensions to biopolymer molecules in solution, such as EPS or mucin. Consequently, they may represent the elongation and breaking of biopolymer links holding the probiotics and mucin together.

For LI05, the average contour lengths were around twice greater than those observed for LGG (Fig. 2c). For instance, the L_C values were 95.1 ± 7.7 nm *vs* 66.1 ± 3.5 nm in GA, 206 ± 13 nm *vs* 98.0 ± 7.9 nm in BS, and 112.9 ± 6.6 nm *vs* 67.3 ± 5.9 nm in buffer solution for LI05 and LGG, respectively. This effect may be due to differences in the nature of the biopolymer molecules or structures on the surfaces of the different probiotic cells. Nevertheless, the impact of gastric acids and bile salts on the L_C values of LI05 followed a similar general trend as observed for LGG. Again, the frequency distribution curves showed that the majority of rupture lengths were below 200 nm in all of the samples. However, there were an appreciable number of higher rupture lengths in the LI05 samples containing bile salts. This result suggests that the presence of the bile salts may have altered the structure of the mucus layer and/or the surfaces of the probiotics.

3.2.3. Rupture force

Rupture force refers to the maximum force required for the detachment of probiotic cells from the AFM tips, which directly relates to the adhesion strength of the probiotics. For both probiotics, the rupture force decreased when they were dispersed in gastric acid solution but increased when they were dispersed in bile salt solution (Fig. 2d). The frequency curves show that the majority of rupture forces were relatively weak (<0.2 nN) in gastric acids for both LGG and LI05. Conversely, there was an appreciable population of relatively strong rupture forces (>1.0 nN) observed in the presence of bile salts. These results suggest that the different gastrointestinal constituents had different effects on the interactions between the probiotics and mucin: the gastric acids weakened the interactions, whereas the bile salts strengthened them.

3.3. Microstructure analysis: AFM and SEM images

Previous studies have shown that changes in solution conditions (such as pH) may affect the morphology of bacteria surfaces (Wetzel and McBride, 2020). For this reason, the morphology of the two strains was evaluated using AFM and SEM under different simulated GIT conditions (Fig. 3). The LGG cells had an oblong ("sausage-like") shape, whereas the LI05 cells had a spherical shape with some evidence of proliferation. For the probiotics in the buffer solutions, the SEM images showed that the surfaces of the LGG cells were relatively rough (Fig. 3a), whereas the surfaces of the LI05 cells were relatively smooth (Fig. 3c). The morphology and interactions of the cells clearly depended on the nature of the gastrointestinal fluids they were suspended in (Fig. 3b and d). For LGG, there was a limited amount of clumping of the probiotic cells suspended in the buffer solutions, with some evidence of a layer of extracellular material partially surrounding the cells. After the addition of gastric acids, there was still considerable clumping but no evidence of the extracellular material. In contrast, after the addition of bile salts, there was still clumping but also evidence of a thick layer of extracellular material surrounding the probiotic cells. For LI05, the cells in the buffer solution appeared to be strongly associated with each other. After the addition of either gastric acids or bile salts there appeared to be some dissociation of the cells. In this case, there appeared to be no evidence of an extracellular layer around the probiotic cells.

3.4. Detection of EPS on the bacterial surface

EPS are known to play an important role in the adhesion of bacterial cells to surfaces (Sun et al., 2007). Previous research has indicated that the EPS of some probiotics may increase their viability during GIT by acting like a protective layer against harsh conditions, such as the low pH of the stomach and the presence bile salts and pancreatic enzymes in the small intestine (Lebeer et al., 2011). Thus, EPS are an adaptation factor of LGG that enhances its survival and persistence inside the host (Lebeer et al., 2011). Once the EPS-producing bacteria arrive in the colon, these surface macromolecules interact with the intestinal mucosa (Castro-Bravo et al., 2018). EPS can enhance the hydrophobicity of the surfaces of the bacterial cell and increase the binding ability of the bacteria to the intestinal mucosa (Sun et al., 2007). For this reason, we measured the EPS concentrations in the different probiotics. The EPS on the surfaces of the probiotic cells were quantified using ELISA. The concentrations of EPS on the surfaces of the LGG and LI05 cell did not change appreciably under different gastrointestinal conditions: GA, BS, and control, with no statistically significant difference being observed (Fig. 4a).

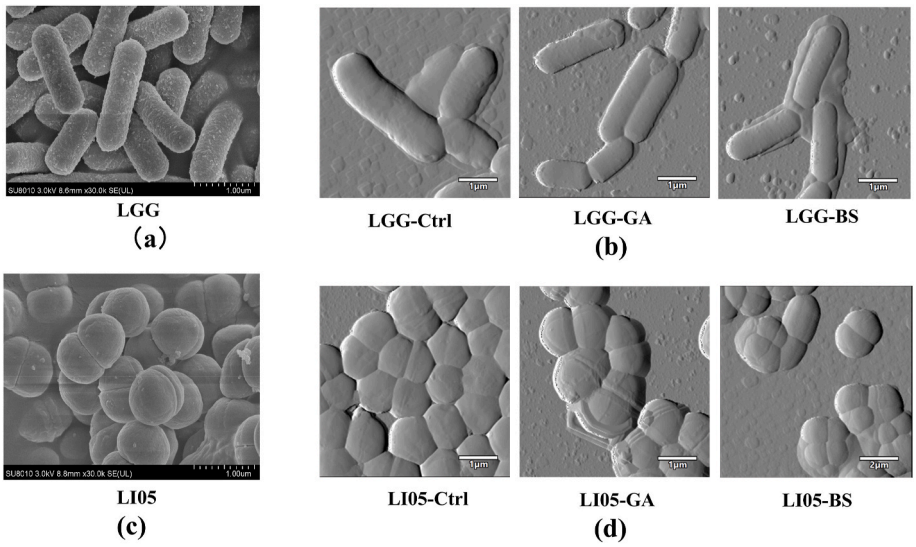

Fig. 3. Morphology change of LGG and LI05 in different conditions. Scanning electron microscopy was used to visualize LGG (a) and *P. pentosaceus* LI05 (c) cells. Atomic force microscopy was used to visualize LGG (b) and *P. pentosaceus* LI05 under exposure to PBS, GA and BS (d). Ctrl, GA and BS represent different groups in the conditions of PBS, gastric acid and bile salts.

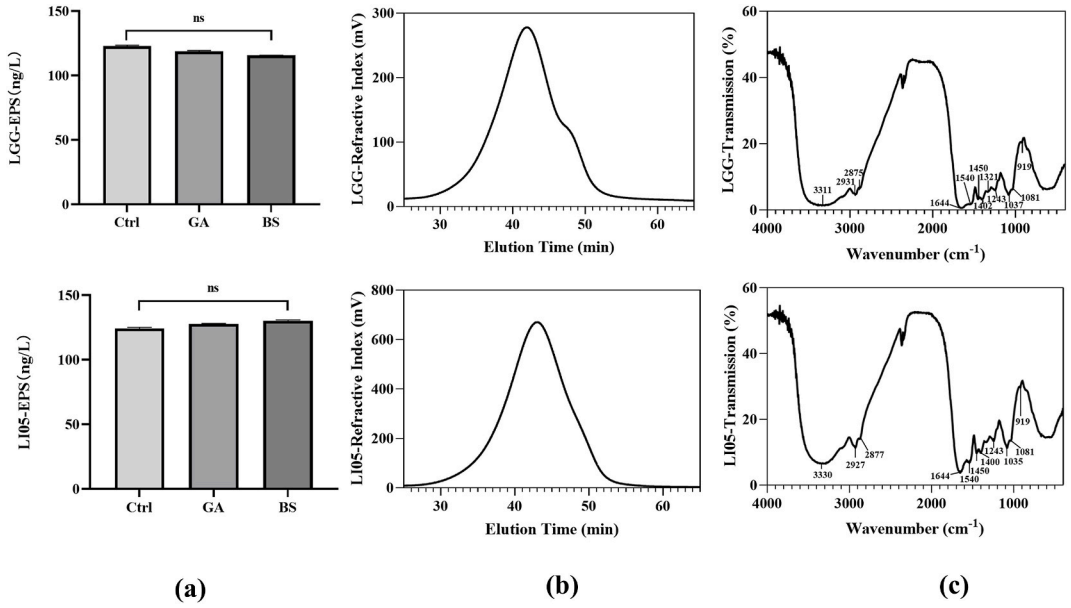

Fig. 4. Characterization of EPS on bacterial surface. (a) The change of extracellular polysaccharides concentration of the two probiotic strains was measured under exposure to gastric acids (GA), bile salts (BS), or PBS (Ctrl). The boxes and error bars represent means ± SEM. (b) Gel purification chromatography of EPS. (c) FT-IR transmission absorption spectrum of EPS.

3.5. Determination of molecular weight and FT-IR spectroscopy analysis

In this section, the functional groups in EPS of both LGG and LI05 were determined by FT-IR spectroscopy. Moreover, the EPS was purified and their molecular weight was measured. Results in Fig. 4b show gel purification chromatography of EPS from the LGG and LI05. LGG contains EPS with the molecular weight 27,229 Da, 14,479 Da, 12,130 Da, 10,372 Da, 7880 Da and 6079 Da, while the EPS of LI05 molecular weight 47,763 Da, 31,127 Da, 17682 Da, 11,985 Da and 10,112 Da (Table 1), indicating the molecular weight of EPS in LI05 is much higher than that in LGG. Fig. 5c displays the FT-IR transmission absorption spectrum of the EPS over the range 4000–400 cm^{-1}. In LGG, the intense and broad peak at 3311 cm^{-1}, a typical absorption band for polysaccharides, represented the O–H stretching vibration from the hydroxyl groups in EPS. The absorption peaks at 2931 cm^{-1} and 2875 cm^{-1} may be attributed to C–H stretching vibration, while that at 1644 cm^{-1} was due to water of crystallization. The absorption peak at 1540 cm^{-1} may due to C═O stretching vibration, while that at 1450 cm^{-1} may be attributed to C–H variable angle vibration and at 1402 cm^{-1} may because of C═O symmetric stretching vibration (Boulet et al., 2007). The spectral wavenumber of 1400–800 cm^{-1}, commonly known as the fingerprint region, is sensitive to carbohydrate type and structure

Table 1
Molecular weight of EPS of LGG and LI05 cells.

Probiotics	Molecular weight (Da)
LGG	27,229,14,479,12,130,10,372,7880,6079
LI05	47,763,31,127,17,682,11,985,10,112

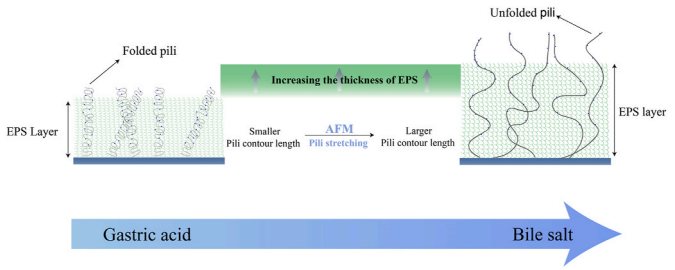

Fig. 5. Potential mechanism of mucoadhesion change under exposure to gastric acids and bile salts. When the probiotics were exposed to gastric acid, the EPS layer becomes more condensed and make the pili more folded. Under bile salt conditions, changes in EPS structure increase its interactions with mucin, and the pili were partially released.

configuration (Gulamhusein et al., 2016). There are absorption peaks at 1321 cm^{-1}, 1243 cm^{-1} and 1037 cm^{-1}, which may be due to O–H variable angle vibration. The absorption peak at 1081 cm^{-1} due to C–O stretching vibration, while that at 919 cm^{-1}, which may be attributed to the asymmetric ring stretching vibration of pyran ring. As for LI05, the FT-IR transmission absorption spectrum of EPS was very close to LGG, in terms of both the position of absorption peaks and the corresponding functional groups.

4. Potential mechanisms of action

A candidate probiotic should meet the criteria of high tolerance to harsh conditions and the ability to colonize the intestine (Valdés-Varela et al., 2018). Gastric acids and bile salts are two of the main constituents in the GIT that are unfavorable to probiotic survival, and which may significantly influence the beneficial effects provided by probiotics. In this study, we evaluated the viscosity, ζ-potentials, morphology, and adhesive properties of probiotics when exposed to gastric acids and bile salts, as well as molecular weight and functional groups of the EPS, to explore the molecular mechanisms of adhesion of LGG and LI05.

The analysis of the shear viscosity *versus* shear rate profiles of the probiotic suspensions provided some valuable insights (Fig. 1b and c). All the suspensions had a high viscosity at low shear rates and exhibited distinct shear thinning behavior, with the shear viscosity decreasing by orders of magnitude as the shear rate was increased. This effect may have been due to entanglement of exopolysaccharides and adhesion of probiotics in the suspensions. As the shear rate was increased, the polysaccharides became increasingly unentangled and the probiotics became dissociated from each other. Interestingly, the LGG samples in BS had a higher shear viscosity than the controls at intermediate shear rates, which may attribute to increase rupture forces (as measured by AFM) required to dissociate the clumps of bacteria. However, there was actually a decrease in the rupture forces for the LGG samples containing gastric acids compared to the control, while the viscosity did not decrease. For LI05, no statistical differences in the shear viscosity profiles were observed for the probiotic suspensions containing different gastrointestinal constituents. This suggests that the bile salts and gastric acids did not have a major impact on the molecular structure of the EPS or the clumping of these probiotic cells. Since LGG cells are rod-shaped whereas LI05 cells are spheroidal, this may also affect their viscosity when exposed to different shear forces.

The surface layers of probiotic cells are composed of macromolecules containing carboxylate, phosphate, and amino functional groups, which can undergo pH-dependent ionization. Consequently, different environmental conditions can confer electrostatic charges to the surfaces of probiotic cells (Halder et al., 2015; Wilson et al., 2001). Both gram-positive and gram-negative bacterial surfaces contain acidic and basic functional groups (Hong and Brown, 2006). The surface charges on bacterial cells affect their electrostatic characteristics and therefore their adhesion and aggregation behavior (Hong and Brown, 2008). Both probiotics were negatively charged under all conditions used in this study but their magnitudes depended on probiotic type and gastrointestinal fluid composition (Fig. 1d and e). Compared to the control, the ζ-potential of LGG became slightly more negative when exposed to gastric acids and less negative when exposed to bile salts (Fig. 1d). However, the changes in ζ-potential were relatively small and not statistically different. In buffer solution, the ζ-potential on the LI05 cells was less negative than that of the LGG cells, which suggests there were some differences in surface compositions. In the case of the LI05 cells, there was a significant increase in the magnitude of the negative charge after addition of both the gastric acids and bile salts (Fig. 1e), which is indicative of a change in the surface properties. There appeared to be no correlation between the electrical characteristics of the probiotics and their adhesion properties. For instance, the trends in the ζ-potential data with gastrointestinal fluids are different to the trends in the rupture properties. These results suggest that the electrical properties of the probiotics did not play a major role in determining their mucoadhesive properties.

EPS play an important role in determining the overall mucoadhesive properties of bacterial cells (Sun et al., 2007). As shown in Fig. 4, the quantity of EPS within the surface layers of the two probiotics did not change when they were exposed to different *in vitro* conditions. Molecular weight of EPS may affect the rupture length. The larger the molecular weight is, the longer the molecular chain is likely to be. The more branch chains are, the more adhesion sites are supposed to be. It may explain the fact that the rupture length in LI05 group in Fig. 2c is longer than that in LGG group. However, the rupture force of the LGG and LI05 is very close (Fig. 2d), since their functional groups of EPS are not significantly different. As we did observe differences in their mucoadhesive properties, we inferred that the molecular structures and spatial conformation (rather than the concentrations) of the EPS may play important roles. The bile salts may have interacted with the surfaces of the probiotics and altered the structural organization of the EPS. Our electron microscopy images appeared to show changes in the structural organization of the extracellular material around the probiotic cells after bile salt addition (Fig. 3).

Change of structure of EPS affect the mucoadhesion of probiotics as shown in Fig. 2, where we directly measured the adhesive forces acting between the probiotics and mucin using an AFM method. Fig. 2a shows the adhesion curves between LGG/LI05 and mucin. The zigzag patterns observed in the retraction curves may suggest the formation of a molecular zipper-like behavior between the mucin and pili (Tripathi et al., 2013). When the probiotics were exposed to gastric acids, the EPS layer became more condensed so that the pili became more folded, which was not conducive to the pili adhering to the mucin (Lebeer et al., 2009). Moreover, condensation of the EPS layer may have reduced its ability to directly contact with the mucin molecules. In bile salt conditions, the changes in EPS structure have increased its interactions with mucin, and the pili may have been at least partially liberated, thereby increasing the accessibility of the pili to the mucin-coated AFM tips, thereby increasing mucoadhesion. Overall, when exposed to bile salts, the number of contact points between the probiotic surfaces and mucin increased, which would account for the observed increase in rupture forces (Fig. 5).

Based on these results, we can infer that the mucoadhesive forces exhibited by LGG or LI05 cells are quite weak under simulated gastric conditions and so we would not expect them to strongly adhere to the stomach lining. In contrast, when the probiotics are exposed to bile salts and neutral pH conditions, the mucoadhesive forces become strong, which would increase their tendency to adhere and colonize the intestinal walls.

5. Conclusions

Our study investigated the effects of a simulated gastrointestinal environment on the mucoadhesive properties of LGG and LI05 cells.

Both types of probiotics had a relatively low negative charge under simulated stomach and small intestine conditions, which did not depend strongly on GIT region. The probiotic suspensions were highly viscous and exhibited strong shear-thinning behavior, which was attributed to the production of EPS and the clumping of the cells. The addition of bile salts increased the apparent shear viscosity of the LGG suspensions, which may have been due to changes in the production of structural organization of EPS or due to increased clumping of the cells. ELISA analysis indicated that the total concentration of EPS did not change under different gastrointestinal conditions. However, the molecular weight of EPS may affect the rupture length of the probiotics and the mucin. Electron microscopy analysis indicated that there were differences in the nature of the extracellular material surrounding the probiotics depending on cell type and gastrointestinal conditions. After bile salt addition, a thick open layer of extracellular material was observed around the probiotic cells (especially for LGG). This change in EPS structure may have increased mucoadhesion by increasing the exposure of pili and by increasing the strength of EPS-mucin interactions. In contrast, after exposure to gastric acids, the EPS layer around the probiotics became thinner and denser. In this case, the change in EPS structure may have reduced the number of pili exposed or reduced the strength of EPS-mucin interactions.

Overall, this study provides valuable new information about the effect of gastric acid and bile salts on probiotic EPS, which contribute to a better understanding of the mucoadhesive behavior of the probiotics in the GIT.

CRediT authorship contribution statement

Yanmeng Lu: Formal analysis, Methodology, Writing – original draft, Writing – review & editing. **Shengyi Han:** Methodology, Writing – original draft, Writing – review & editing. **Shuobo Zhang:** Data curation. **Kaicen Wang:** Writing – review & editing. **Longxian Lv:** Writing – review & editing. **David Julian McClements:** Writing – review & editing. **Hang Xiao:** Writing – review & editing. **Björn Berglund:** Writing – review & editing. **Mingfei Yao:** Conceptualization, Project administration, Funding acquisition, Supervision, Writing – review & editing. **Lanjuan Li:** Conceptualization, Project administration, Funding acquisition, Supervision, Writing – review & editing.

Declaration of competing interest

The authors declare that they have no known competing financial interests or personal relationships that could have appeared to influence the work reported in this paper.

Acknowledgments

This work was supported by the Major Program of the National Natural Science Foundation of China (81790631) and the National Natural Science Foundation of China (32001683).

References

Boulet, J.C., Williams, P., Doco, T., 2007. A Fourier transform infrared spectroscopy study of wine polysaccharides. Carbohydr. Polym. 69 (1), 79–85. https://doi.org/10.1016/j.carbpol.2006.09.003.

Bramhachari, P.V., Dubey, S.K., 2006. Isolation and characterization of exopolysaccharide produced by Vibrio harveyi strain VB23. Lett. Appl. Microbiol. 43 (5), 571–577. https://doi.org/10.1111/j.1472-765X.2006.01967.x.

Brodkorb, A., Egger, L., Alminger, M., Alvito, P., Assuncao, R., Ballance, S., Bohn, T., Bourlieu-Lacanal, C., Boutrou, R., Carriere, F., Clemente, A., Corredig, M., Dupont, D., Dufour, C., Edwards, C., Golding, M., Karakaya, S., Kirkhus, B., Le Feunteun, S., Lesmes, U., Macierzanka, A., Mackie, A.R., Martins, C., Marze, S., McClements, D.J., Menard, O., Minekus, M., Portmann, R., Santos, C.N., Souchon, I., Singh, R.P., Vegarud, G.E., Wickham, M.S.J., Weitschies, W., Recio, I., 2019. INFOGEST static in vitro simulation of gastrointestinal food digestion. Nat. Protoc. 14 (4), 991–1014. https://doi.org/10.1038/s41596-018-0119-1.

Burgain, J., Scher, J., Lebeer, S., Vanderleyden, J., Corgneau, M., Guerin, J., Caillet, C., Duval, J.F., Francius, G., Gaiani, C., 2015. Impacts of pH-mediated EPS structure on probiotic bacterial pili-whey proteins interactions. Colloids Surf. B Biointerfaces 134, 332–338. https://doi.org/10.1016/j.colsurfb.2015.06.068.

Cao, F., Liang, M., Liu, J., Liu, Y., Renye Jr., J.A., Qi, P.X., Ren, D., 2021. Characterization of an exopolysaccharide (EPS-3A) produced by *Streptococcus thermophilus* ZJUIDS-2-01 isolated from traditional yak yogurt. Int. J. Biol. Macromol. 192, 1331–1343. https://doi.org/10.1016/j.ijbiomac.2021.10.055.

Castro-Bravo, N., Wells, J.M., Margolles, A., Ruas-Madiedo, P., 2018. Interactions of surface exopolysaccharides from *bifidobacterium* and *lactobacillus* within the intestinal environment. Front. Microbiol. 9, 2426. https://doi.org/10.3389/fmicb.2018.02426.

Ciszek-Lenda, M., 2011. Biological functions of exopolysaccharides from probiotic bacteria. Cent. Eur. J. Immunol. 36 (1), 51–55.

Gulamhusein, A.F., Eaton, J.E., Tabibian, J.H., Atkinson, E.J., Juran, B.D., Lazaridis, K. N., 2016. Duration of inflammatory bowel disease is associated with increased risk of cholangiocarcinoma in patients with primary sclerosing cholangitis and IBD. Am. J. Gastroenterol. 111 (5), 705–711. https://doi.org/10.1038/ajg.2016.55.

Halder, S., Yadav, K.K., Sarkar, R., Mukherjee, S., Saha, P., Haldar, S., Karmakar, S., Sen, T., 2015. Alteration of Zeta potential and membrane permeability in bacteria: a study with cationic agents. SpringerPlus 4, 672. https://doi.org/10.1186/s40064-015-1476-7.

Han, S., Lu, Y., Xie, J., Fei, Y., Zheng, G., Wang, Z., Liu, J., Lv, L., Ling, Z., Berglund, B., Yao, M., Li, L., 2021. Probiotic gastrointestinal transit and colonization after oral administration: a long journey. Front Cell Infect Microbiol 11, 609722. https://doi.org/10.3389/fcimb.2021.609722.

Hong, Y., Brown, D.G., 2006. Cell surface acid-base properties of *Escherichia coli* and *Bacillus brevis* and variation as a function of growth phase, nitrogen source and C:N ratio. Colloids Surf. B Biointerfaces 50 (2), 112–119. https://doi.org/10.1016/j.colsurfb.2006.05.001.

Hong, Y., Brown, D.G., 2008. Electrostatic behavior of the charge-regulated bacterial cell surface. Langmuir 24 (9), 5003–5009. https://doi.org/10.1021/la703564q.

Johansson, M.E., Larsson, J.M., Hansson, G.C., 2011. The two mucus layers of colon are organized by the MUC2 mucin, whereas the outer layer is a legislator of host-microbial interactions. Proc. Natl. Acad. Sci. U. S. A. 108 (Suppl. 1), 4659–4665. https://doi.org/10.1073/pnas.1006451107. Suppl 1.

Johansson, M.E., Phillipson, M., Petersson, J., Velcich, A., Holm, L., Hansson, G.C., 2008. The inner of the two Muc2 mucin-dependent mucus layers in colon is devoid of bacteria. Proc. Natl. Acad. Sci. U. S. A. 105 (39), 15064–15069. https://doi.org/10.1073/pnas.0803124105.

Kankainen, M., Paulin, L., Tynkkynen, S., von Ossowski, I., Reunanen, J., Partanen, P., Satokari, R., Vesterlund, S., Hendrickx, A.P., Lebeer, S., De Keersmaecker, S.C., Vanderleyden, J., Hämäläinen, T., Laukkanen, S., Salovuori, N., Ritari, J., Alatalo, E., Korpela, R., Mattila-Sandholm, T., Lassig, A., Hatakka, K., Kinnunen, K.T., Karjalainen, H., Saxelin, M., Laakso, K., Surakka, A., Palva, A., Salusjärvi, T., Auvinen, P., de Vos, W.M., 2009. Comparative genomic analysis of *Lactobacillus rhamnosus* GG reveals pili containing a human- mucus binding protein. Proc. Natl. Acad. Sci. U. S. A. 106 (40), 17193–17198. https://doi.org/10.1073/pnas.0908876106.

Konieczna, C., Słodziński, M., Schmidt, M.T., 2018. Exopolysaccharides produced by *Lactobacillus rhamnosus* KL 53A and *Lactobacillus casei* fyos affect their adhesion to enterocytes. Pol. J. Microbiol. 67 (3), 273–281. https://doi.org/10.21307/pjm-2018-032.

Kumar, A., Kumar, D., 2015. Characterization of *Lactobacillus* isolated from dairy samples for probiotic properties. Anaerobe 33, 117–123. https://doi.org/10.1016/j.anaerobe.2015.03.004.

Lebeer, S., Claes, I.J., Verhoeven, T.L., Vanderleyden, J., De Keersmaecker, S.C., 2011. Exopolysaccharides of *Lactobacillus rhamnosus* GG form a protective shield against innate immune factors in the intestine. Microb Biotechnol 4 (3), 368–374. https://doi.org/10.1111/j.1751-7915.2010.00199.x.

Lebeer, S., Verhoeven, T.L., Francius, G., Schoofs, G., Lambrichts, I., Dufrêne, Y., Vanderleyden, J., De Keersmaecker, S.C., 2009. Identification of a gene cluster for the biosynthesis of a long, galactose-rich exopolysaccharide in *Lactobacillus rhamnosus* GG and functional analysis of the priming glycosyltransferase. Appl. Environ. Microbiol. 75 (11), 3554–3563. https://doi.org/10.1128/aem.02919-08.

Lv, L.X., Li, Y.D., Hu, X.J., Shi, H.Y., Li, L.J., 2014. Whole-genome sequence assembly of *Pediococcus pentosaceus* LI05 (CGMCC 7049) from the human gastrointestinal tract and comparative analysis with representative sequences from three food-borne strains. Gut Pathog 6, 36. https://doi.org/10.1186/s13099-014-0036-y.

Nishiyama, K., Sugiyama, M., Mukai, T., 2016. Adhesion properties of lactic acid bacteria on intestinal mucin. Microorganisms 4 (3). https://doi.org/10.3390/microorganisms4030034.

Proft, T., Baker, E.N., 2009. Pili in Gram-negative and Gram-positive bacteria - structure, assembly and their role in disease. Cell. Mol. Life Sci. 66 (4), 613–635. https://doi.org/10.1007/s00018-008-8477-4.

Rahbar Saadat, Y., Yari Khosroushahi, A., Pourghassem Gargari, B., 2019. A comprehensive review of anticancer, immunomodulatory and health beneficial effects of the lactic acid bacteria exopolysaccharides. Carbohydr. Polym. 217, 79–89. https://doi.org/10.1016/j.carbpol.2019.04.025.

Reale, A., Di Renzo, T., Rossi, F., Zotta, T., Iacumin, L., Preziuso, M., Parente, E., Sorrentino, E., Coppola, R., 2015. Tolerance of *Lactobacillus casei, Lactobacillus paracasei* and *Lactobacillus rhamnosus* strains to stress factors encountered in food processing and in the gastro-intestinal tract. LWT - Food Sci. Technol. (Lebensmittel-Wissenschaft -Technol.) 60 (2), 721–728. https://doi.org/10.1016/j.lwt.2014.10.022.

Shi, D., Lv, L., Fang, D., Wu, W., Hu, C., Xu, L., Chen, Y., Guo, J., Hu, X., Li, A., Guo, F., Ye, J., Li, Y., Andayani, D., Li, L., 2017. Administration of *Lactobacillus salivarius* LI01 or *Pediococcus pentosaceus* LI05 prevents CCl(4)-induced liver cirrhosis by protecting the intestinal barrier in rats. Sci. Rep. 7 (1), 6927. https://doi.org/10.1038/s41598-017-07091-1.

Sun, J., Le, G.W., Shi, Y.H., Su, G.W., 2007. Factors involved in binding of *Lactobacillus plantarum* Lp6 to rat small intestinal mucus. Lett. Appl. Microbiol. 44 (1), 79–85. https://doi.org/10.1111/j.1472-765X.2006.02031.x.

Tripathi, P., Beaussart, A., Alsteens, D., Dupres, V., Claes, I., von Ossowski, I., de Vos, W. M., Palva, A., Lebeer, S., Vanderleyden, J., Dufrêne, Y.F., 2013. Adhesion and nanomechanics of pili from the probiotic *Lactobacillus rhamnosus* GG. ACS Nano 7 (4), 3685–3697. https://doi.org/10.1021/nn400705u.

Valdés-Varela, L., Gueimonde, M., Ruas-Madiedo, P., 2018. Probiotics for prevention and treatment of *Clostridium difficile* infection. Adv. Exp. Med. Biol. 1050, 161–176. https://doi.org/10.1007/978-3-319-72799-8_10.

Van Tassell, M.L., Miller, M.J., 2011. *Lactobacillus* adhesion to mucus. Nutrients 3 (5), 613–636. https://doi.org/10.3390/nu3050613.

von Ossowski, I., Reunanen, J., Satokari, R., Vesterlund, S., Kankainen, M., Huhtinen, H., Tynkkynen, S., Salminen, S., de Vos, W.M., Palva, A., 2010. Mucosal adhesion properties of the probiotic *Lactobacillus rhamnosus* GG SpaCBA and SpaFED pilin subunits. Appl. Environ. Microbiol. 76 (7), 2049–2057. https://doi.org/10.1128/aem.01958-09.

Wetzel, D., McBride, S.M., 2020. The impact of pH on *Clostridioides difficile* sporulation and physiology. Appl. Environ. Microbiol. 86 (4) https://doi.org/10.1128/aem.02706-19.

Wilson, W.W., Wade, M.M., Holman, S.C., Champlin, F.R., 2001. Status of methods for assessing bacterial cell surface charge properties based on zeta potential measurements. J. Microbiol. Methods 43 (3), 153–164. https://doi.org/10.1016/s0167-7012(00)00224-4.

Xu, Y., Zhu, J., Feng, B., Lin, F., Zhou, J., Liu, J., Shi, X., Lu, X., Pan, Q., Yu, J., Zhang, Y., Li, L., Cao, H., 2021. Immunosuppressive effect of mesenchymal stem cells on lung and gut CD8(+) T cells in lipopolysaccharide-induced acute lung injury in mice. Cell Prolif 54 (5), e13028. https://doi.org/10.1111/cpr.13028.

Yao, M., Wu, J., Li, B., Xiao, H., McClements, D.J., Li, L., 2017. Microencapsultion of *Lactobacillus salivarious* Li01 for enhanced storage viability and targeted delivery to gut microbiota. Food Hydrocolloids 72, 228–236. https://doi.org/10.1016/j.foodhyd.2017.05.033.

Yao, M.F., Xie, J.J., Du, H.J., McClements, D.J., Xiao, H., Li, L.J., 2020. Progress in microencapsulation of probiotics: a review. Compr. Rev. Food Sci. Food Saf. 19 (2), 857–874. https://doi.org/10.1111/1541-4337.12532.

Zhou, Y., Cui, Y., Qu, X., 2019. Exopolysaccharides of lactic acid bacteria: structure, bioactivity and associations: a review. Carbohydr. Polym. 207, 317–332. https://doi.org/10.1016/j.carbpol.2018.11.093.

Zmora, N., Zilberman-Schapira, G., Suez, J., Mor, U., Dori-Bachash, M., Bashiardes, S., Kotler, E., Zur, M., Regev-Lehavi, D., Brik, R.B., Federici, S., Cohen, Y., Linevsky, R., Rothschild, D., Moor, A.E., Ben-Moshe, S., Harmelin, A., Itzkovitz, S., Maharshak, N., Shibolet, O., Shapiro, H., Pevsner-Fischer, M., Sharon, I., Halpern, Z., Segal, E., Elinav, E., 2018. Personalized gut mucosal colonization resistance to empiric probiotics is associated with unique host and microbiome features. Cell 174 (6), 1388–1405. https://doi.org/10.1016/j.cell.2018.08.041 e1321.